CSCE Annual Conference

Growing with youth – Croître avec les jeunes

Laval (Greater Montreal)

June 12 - 15, 2019

VALUE OF STRUCTURAL HEALTH MONITORING OF A CORRODED REINFORCED CONCRETE BEAM

Mao, Zoe[1,2], Wegner, Leon.[1]
[1] University of Saskatchewan, Canada
[2] zoe.mao@usask.ca

Abstract: Corrosion is a major factor that causes degradation of reinforced concrete structural elements, especially in cold regions where de-icing salts are used extensively. It is difficult to assess the remaining capacity of a corroded reinforced concrete member based on visual inspections alone, and therefore to determine whether the member has an adequate level of safety. An appropriate structural health monitoring (SHM) system can provide real-time information about a structure's actual condition, thereby allowing a determination of its level of safety and whether remedial measures are required or the service life can be extended, resulting in a savings of replacement costs. Quantification of the economic benefits of SHM systems with different levels of sophistication has not been studied extensively but is one of the critical factors in selecting the optimum SHM system. This paper describes the results of a laboratory-based experimental study. The first objective of this study was to evaluate the effectiveness of a surface strain-based SHM technique for determining the bending moment capacity of a corroded reinforced concrete beam and its remaining level of safety in terms of the reliability index. The second objective was to assess the effect of using SHM information with different levels of uncertainty on the resulting reliability index and life cycle costs. Different monitoring schemes were implemented, consisting of combinations of data sets from different measurement devices (electrical strain gauges, a digital image correlation (DIC) system, and a cover meter). The value of implementing a more precise SHM system is demonstrated through increased reliability indexes and reduced life-cycle costs for the beams.

1 INTRODUCTION

1.1 Background

Corrosion is a major factor that causes structural degradation of reinforced concrete elements. This is because of the loss of effective cross-sectional area of the steel reinforcing bars, as well as the loss of bond between rebar and concrete due to corrosion (Zhang et al. 2013). Reinforced concrete structures in cold regions like Canada are more prone to corrosion damage due to the use of de-icing salts. To ensure public safety, it is important to monitor the deteriorating condition of a structural element in order to decide when to repair or replace it. Currently, most structural evaluations rely largely on visual inspections, which are performed at regular time intervals. Considering the increasing number of aging structures globally, and the limitations of visual inspections, this current approach seems inadequate. The U.S. Federal Highway Administration (FHWA) conducted a research study to investigate the reliability of routine and in-depth visual inspections on highway bridges. The results showed that routine inspections were completed with

large variability, and in-depth inspections based on visual inspection only were not sufficient to identify specific types of defects (FHWA 2001).

Structural health monitoring (SHM) techniques provide real time monitoring and diagnoses of a structure's condition. The implementation of SHM systems allows the structure's maintenance and replacement schedule to be changed from a time-based approach to a condition-based approach, which is more reliable, efficient and cost effective (Farrar and Worden 2007). Various SHM techniques have been developed in the last 30 to 40 years (Qin et al. 2015). One of the ways to classify the various methods is according to the level of information provided by the SHM systems (Rytter 1993): Level 1 identifies the presence of damage; Level 2 specifies the location of the damage; Level 3 indicates the severity of the damage, along with the location; and Level 4 provides an estimate of the remaining service life, in addition to the information provided by Levels 1 through 3. Most of the current SHM systems are Level 2 and require advanced numerical analyses such as fast Fourier transform, eigenvalue analysis or finite element analysis.

Christensen et al. (2011) proposed a theoretical SHM method for estimating the bending moment capacity of a reinforced concrete beam that was subject to corrosion. This method estimated the remaining rebar area after corrosion using the measured flexural strain distribution. The remaining load-bearing capacity of the monitored structural member could then be determined. This surface strain-based method is extremely easy to understand, relying on theories of simple structural mechanics. Thus, it is user friendly and cost effective, especially considering the fact that it is a Level 4 SHM system. However, the approach has never been verified experimentally.

In addition to demonstrating the technical feasibility, it is also useful to investigate the effects and costs of implementing SHM systems in order to encourage the adoption of these technologies in practice, as well as to make an optimized selection among different SHM systems. The implementation of an SHM system itself has no effect on the physical condition of a structure. However, data gathered through this system can help to reduce the uncertainty in the prediction of a structure's load-bearing capacity, which can then be used to increase the level of confidence in its safety and reduce its life-cycle costs.

Structural reliability analysis is an approach to quantify and account for the effect of uncertainty on the safety of structures. The reliability index, β, is defined as the difference between the mean resistance and load effect divided by the corresponding standard deviation. Common values for β range from 2 to 4 for structural assessment, and each value corresponds to a particular probability of failure. For instance, a reliability index of 2 corresponds to a probability of failure of 0.02275 (Frangopol and Messervey 2011). Theoretically, the higher the precision of the SHM system being implemented on a structure, the higher the reliability index for the structure.

The reduced uncertainty in estimation provided by an SHM system can also be used to reduce the life-cycle cost (LCC) of a structure, and therefore the extra cost of implementing the system can be justified. Cost is one of the critical parameters to consider when selecting the most appropriate SHM system for a structure (Loupos and Amditis 2017), since any decision made in structural design and management should be a balance of economy and safety (Frangopol and Messervey 2011). The implementation of SHM systems is an extra cost to a structure's original budget. Even though a more sophisticated SHM system will usually cost more, it can also provide a higher level of structural reliability, which may allow a deteriorating structure to remain in service for a longer period of time while keeping the risk of failure within an acceptable range. Christensen et al. (2011) demonstrated the economic value of SHM systems with three different levels of uncertainty using the annual life-cycle cost of a hypothetical beam. However, this approach also has not been verified experimentally.

The objectives of this study were first to verify the technical feasibility of the SHM method proposed by Christensen et al. (2011), and then to demonstrate the economic benefits of implementing SHM techniques

with different levels of sophistication in terms of the life-cycle costs of a reinforced concrete beam subject to corrosion.

1.2 Theoretical Basis of the Surface Strain-based SHM Method

The principles of the surface strain-based SHM method for determining the remaining bending moment capacity of a corroding reinforced concrete beam were first described by Christensen et al. (2011), and may be understood by considering Figure 1. Figure 1 (a) shows a reinforced concrete beam instrumented with two strain gauges attached at mid-span (where the bending moment is the largest) at depths of d_1 and d_2 from the top surface. Readings from these strain gauges, ε_1 and ε_2, can be used to generate a linear strain diagram, as shown in Figure 1 (b). The distance from the top surface to the neutral axis, c, can be found using the similar triangles. If more than two strain gauges are used to increase the reliability of the data, a linear best bit function, obtained, for example, using the least squares method, can be used to determine the neutral axis location.

Based on the principles of mechanics of materials, as long as the beam is within elastic deformation range, the neutral axis will coincide with the centroid of the transformed cross-sectional area. Since concrete has little tensile strength, the tension side of the beam cracks at a low bending moment. After the beam has cracked, the neutral axis remains at a fixed location until the beam exceeds the elastic deformation range. Thus, the transformed reinforcing steel area, A_t, can be found by solving the geometry of the cross-sectional area. The effective bar area can then be calculated from A_t and n, the modular ratio of steel to concrete. Knowing the actual amount of reinforcement left in the corroded beam, the remaining bending moment capacity of the beam can be predicted.

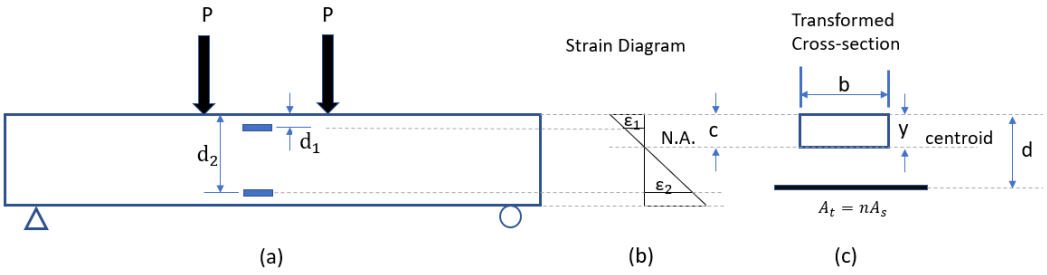

Figure 1: (a) Profile of the beam, showing the location of the two strain gauges; (b) the strain diagram showing the relationship of the similar triangles; and (c) the cracked transformed section used to find centroid

2 EXPERIMENTAL PROGRAM

2.1 Overview

The strain-based SHM technique was tested on three reinforced concrete beams with dimensions of 70×140×2000 mm. A single No. 10 reinforcing bar with a yield strength of 400 MPa was used in each beam, and the mean compressive strength of concrete was 38.27 MPa. After the beams were cured for 28 days, they were subjected to accelerated corrosion to achieve a 10% weight loss of the reinforcing bars in the middle 100 mm section of the beam using the impressed current method. Two four-point loading tests were performed, one before and one after the corrosion, with the maximum load set to remain within the elastic range while exceeding the cracking load. Strain data from each loading test were used to estimate the effective cross-sectional area of the reinforcing bars, as described in the previous section. The estimated reinforcement area from the first loading test was compared to the known area prior to corrosion (100 mm^2). After the second loading test, beams were loaded to failure. Reinforcing bars were extracted

and cleaned by the procedures described in ASTM G1 (ASTM 2017). Following the cleaning, the actual weight losses and remaining diameters were measured and compared to the estimated values.

The configurations of the beams and the set-up of the loading test are illustrated in Figure 2. With this specific experimental design, the impact of loss of bond due to corrosion was minimized. Since corrosion was constrained to occur only in the middle 100 mm section, the rest of the reinforcing bar maintained its original bond strength. The controlled corrosion was achieved by adding 5% sodium chlorides by the weight of cement to the concrete mixture of the target section. The use of the four-point loading set-up created a constant moment region in the middle 200 mm section; therefore, bonding was not required in the corroded section.

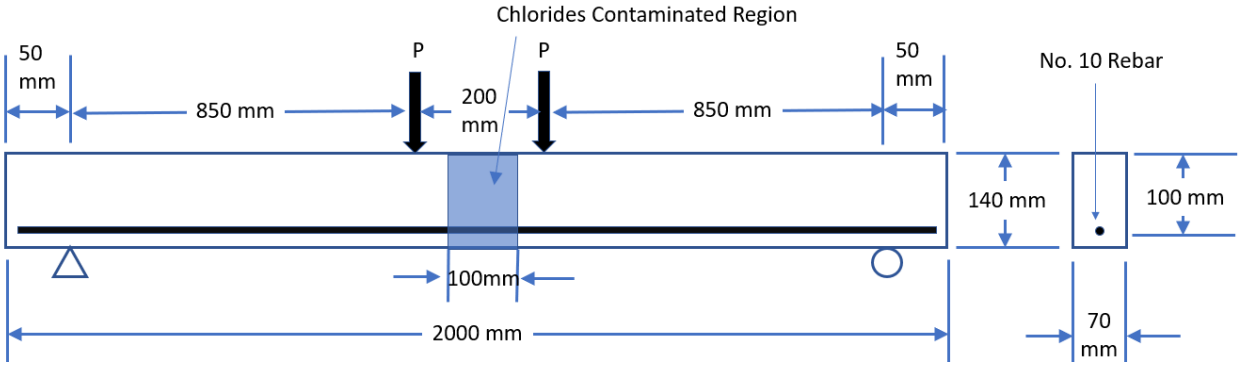

Figure 2: Dimensions of the beams and the set-up of the four-point loading test

2.2 Monitoring Schemes and Equipment

Strain data were acquired using two different techniques: electrical strain gauges and the DIC system. Electrical strain gauges with a 60 mm gauge length (model PL-60-11-3LJCT-F, Tokyo Sokki Kenkjujo Co. Ltd., Japan) were used to even out the non-homogeneous effect of concrete. Four electrical strain gauges were attached at mid-span on one side surface of each beam above the neutral axis (i.e., in the compression zone). The opposite surface was monitored by the DIC system (model VIC-2D 6, Correlated Solutions Inc., US), which is a non-contact optical method that provides in-plane displacements and strains. The DIC system tracks the movement of a speckle pattern on an object's surface using digital images. The strain resolution of the DIC 2D system is within 50 με (Correlated Solutions 2018), which is higher than 5 με provided by the electrical strain gauges (calculated statistically from test results).

Figure 3 shows a beam being monitored by the DIC system and electrical strain gauges during a loading test. The left-hand side surface of the beam is painted with a speckle pattern and is being monitored by the DIC system. The right-hand side has electrical strain gauges attached and is connected to a DAQ system.

In addition to the strain measurements, a cover meter (model Profometer 5+, Proceq SA, Switzerland) with a tolerance of ±2 mm was used to measure the location of reinforcing bars, thus reducing the uncertainty associated with this variable (Proceq 2007).

Four SHM schemes can be developed by using different combinations of the strain measuring equipment and the cover meter, as summarized in Table 1. Each monitoring scheme has different levels of uncertainty associated with measured strain data and reinforcing bar locations. The different levels of uncertainty associated with these variables translates into different levels of uncertainty for the estimated bending moment resistance, and therefore affects the reliability index of the beam.

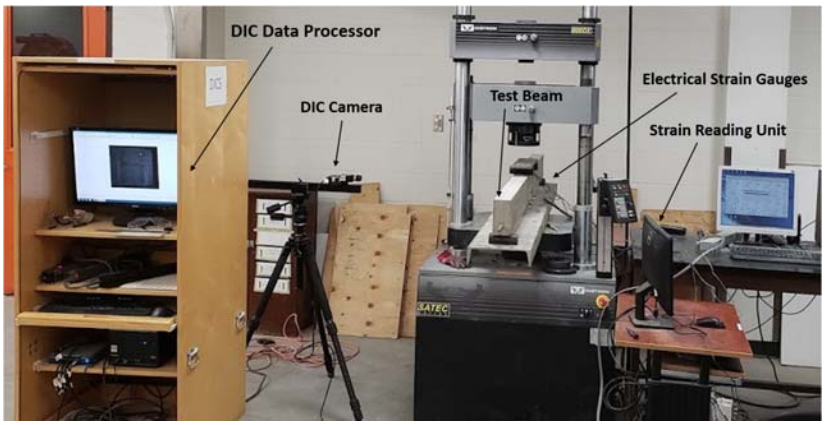

Figure 3: The experimental set-up, showing a beam being monitored by the DIC system and electrical strain gauges during a loading test

Table 1: Instruments used for each SHM scheme

SHM Scheme	Monitoring Equipment
1	Electrical strain gauges
2	Electrical strain gauges + cover meter
3	DIC system
4	DIC system + cover meter

3 EXPERIMENTAL RESULTS

3.1 Effectiveness of the Proposed Strain-based SHM Technique

During the pre-corrosion and post-corrosion loading test of each beam, strain data provided by the DIC and electrical strain gauges (ESGs) were used individually to estimate the neutral axis location. These estimates were compared to theoretical values, which were calculated based on the actual reinforcing bar area and specified dimensions for each beam. A comparison of these results is shown in Table 2. It can be seen that the ESG data resulted in estimates of the neutral axis location that were within 10% of the theoretical values, while the DIC system resulted in estimates within 20%.

Table 2(a): Pre-corrosion load test neutral axis location, measured from the top surface in mm

	Theoretical	ESG	% Diff	DIC	% Diff	Average	% Diff
Beam 1	38.6	41.8	7.8%	32.3	-17.8%	37.0	-4.2%
Beam 2	39.0	42.1	8.7%	39.0	1.0%	40.5	4.9%
Beam 3	38.8	36.7	-5.1%	41.1	6.1%	38.9	0.7%

Table 2(b): Post-corrosion load test neutral axis location, measured from the top surface in mm

	Theoretical	ESG	% Diff	DIC	% Diff	Average	% Diff
Beam 1	37.1	37.8	2.0%	34.5	-7.2%	36.2	-2.5%
Beam 2	37.5	40.6	8.1%	33.8	-10.3%	37.2	-0.7%
Beam 3	37.3	40.3	7.9%	35.4	-5.0%	37.9	1.7%

It is observed that for the same beam, the estimates from the DIC and ESG data consistently lay on opposite sides of the theoretical neutral axis location. This might be due to asymmetrical conditions associated

eccentric loading or supports, or non-uniform cross-sectional properties, and the fact that the two data sets were obtained from the opposite surfaces of the beams. In order to reduce these effects, an average was taken between the two estimates. The average results are within 5% of the theoretical values. A 5% difference in neutral axis location results in approximately 15% difference in cross-sectional area estimation and 4% difference in calculated bending moment capacity.

Table 3 shows the estimated remaining bending moment resistance after corrosion based on averaged neutral axis locations. These values are seen to lie within 5% of the actual failure loads measured at the end of the post-corrosion load tests.

Table 3: Comparison of estimated bending moment resistance based on average neutral axis location and actual bending moment resistance

Beam #	Averaged N.A. (mm)	Estimated Area (mm^2)	Estimated Moment Resistance (kN·m)	Estimated Load Resistance (kN)	Actual Ultimate Load Applied (kN)	% diff
B1	36.2	84.6	5.0	11.7	11.2	-3.8%
B2	37.2	88.3	5.0	11.8	12.4	4.5%
B3	37.9	94.2	5.3	12.4	12.7	2.9%

3.2 Comparison of the Digital Image Correlation System and Electrical Strain Gauges

Figure 4 shows a typical load test result, corresponding to the post-corrosion load test for Beam 2. The graph plots the neutral axis location estimated using DIC data and ESG data with increasing load until failure. It is obvious that there is more noise in the DIC data as compared to the ESG data. This might be due to the poorer precision of the DIC measurements compared to ESGs. Also, the DIC camera measures from a distance, so other factors such as the vibration of the loading machine, dust in the air, and lighting conditions in the lab may also affect the precision of DIC measurements.

The main advantage of using the DIC system is that it provided reliable data even at extreme loads, while the ESGs broke at an applied load of approximately 11 kN due to their lower strain limit (0.002). Concrete ultimate compressive strain is approximately 0.0035, which means any ESGs close to the extreme compressive surface will break before the concrete crushes. ESGs were also found to be unreliable when attached in the tension zone, due to high local strains caused by concrete cracking or corrosion. The side surfaces of the beams used for these tests only provided enough space for four ESGs to be attached in the compression zone. However, the DIC system can monitor strains in both the compression and tension zones. In addition, averaged strain data along any specified line can be extracted at any location by drawing virtual extensometers in the DIC 2D analysis software, as shown in Figure 5.

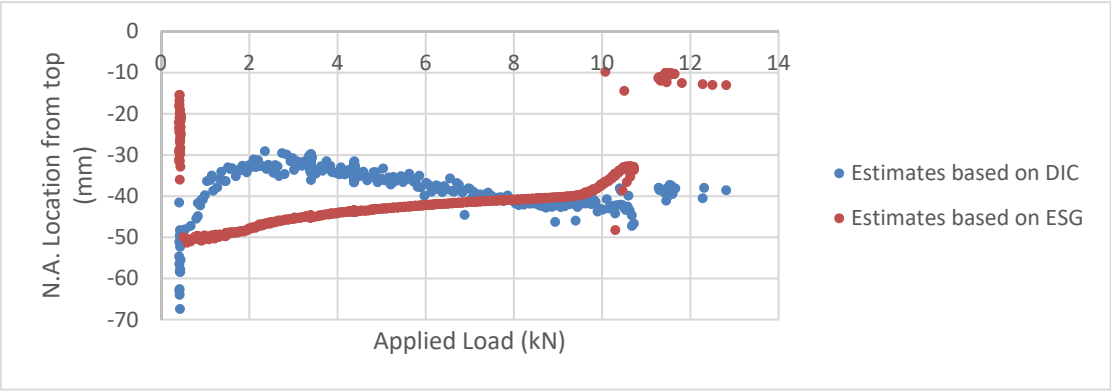

Figure 4: Comparison of DIC and electrical strain gauge data (post-corrosion load test for Beam 2)

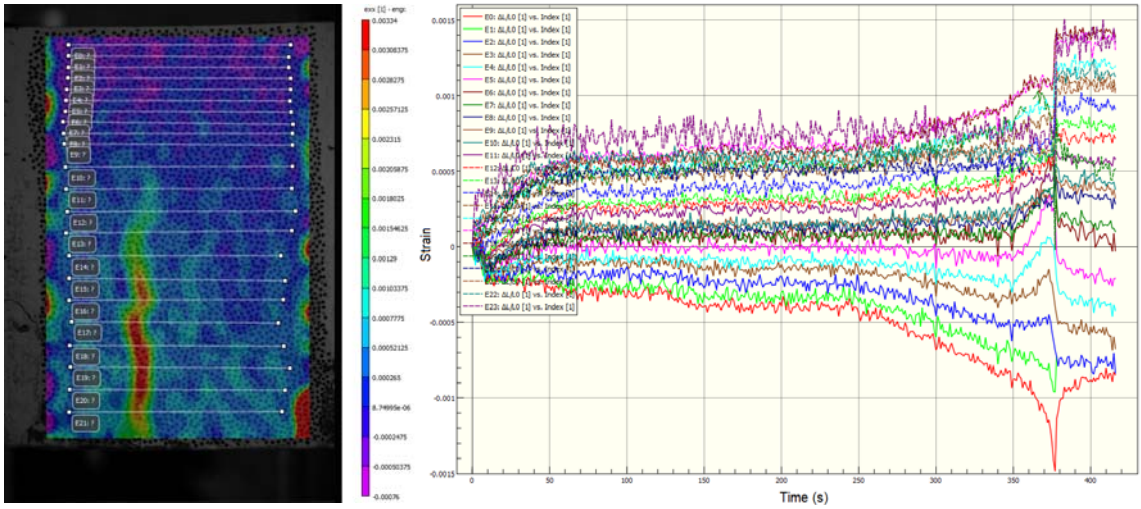

(a) (b)

Figure 5: DIC Analysis from post corrosion load test for Beam 2: (a) strain field on the side surface of the beam, with numerous virtual extensometers defined, and (b) a plot of the average strain along each virtual extensometer as the beam was tested to failure

4 RELIABILITY ANALYSIS

The reliability index, β, is defined as follows (Frangopol and Messervey 2011):

[1] $\beta = \frac{\mu_R - \mu_L}{\sqrt{\sigma_R^2 + \sigma_L^2}}$

where μ_R and μ_L are the mean values of resistance and load effect, respectively, and σ_R and σ_L are the corresponding standard deviations. The reliability index is related to a level of confidence, or the probability that the structure is safe (i.e., resistance > load effect). To design a structure that is absolutely safe is impossible and will not be economically efficient. Therefore, structures are generally designed and evaluated based on a certain level of confidence (Frangopol and Messervey, 2011).

For each beam tested, its reliability index was calculated using the data from each combination of monitoring equipment listed in Table 1. The load effect was taken as 3.215 kN·m, which is equal to the factored design moment capacity calculated based on CSA A23.3-14. For the purpose of this exercise, it was assumed to be known with certainty, and its corresponding standard deviation was set to zero. In a laboratory setting, since the load is applied by a universal test machine, the uncertainty associated with the load is very small. The bending moment resistance, M_u, was calculated based on the estimated neutral axis location and the estimated area of the reinforcement, and its corresponding standard deviation, σ_u, was calculated as an accumulation of the standard deviations of all variables used to calculate the mean beam resistance, assuming all variables were normally distributed and independent (Christensen et al. 2011).

There are two possible ways to estimate the standard deviation for a variable. One is through statistical data, and the other is through the specified tolerance or precision of an instrument. For this exercise, the standard deviation of concrete strength was calculated statistically from the results of several compression tests on concrete cylinder samples. The tolerance for beam height and concrete cover thickness specified by CSA A23.1-14 is ±12 mm, which was assumed to correspond to the 90% confidence limits, which lie

1.645 standard deviations from the mean. A standard deviation of $\frac{12\ \text{mm}}{1.645} = 7.3\ \text{mm}$ was therefore used for these variables. For the strain readings, the statistical method was used.

Table 4 summarizes the reliability indexes obtained using Scheme 1 (electrical strain gauges only), Scheme 2 (electrical strain gauges and cover meter), Scheme 3 (DIC system only), and Scheme 4 (DIC system and cover meter). Without using a cover meter, the standard deviation for the location of the reinforcement is based on the tolerance for concrete cover specified by CSA A23.1-14 of ±12 mm. If a cover meter is used, this value can be reduced to ±2 mm based on the precision of the instrument, assumed to correspond to the 90% confidence limits. Thus, the reliability indexes based on Scheme 2 and 4 are significantly higher than those based on Scheme 1 and 3.

Table 4: Comparison of reliability indexes

		Scheme 1		Scheme 2			Scheme 3		Scheme 4	
Beam #	Mu (kN*m)	σu (kN*m)	β	σu (kN*m)	β	Mu (kN*m)	σu (kN*m)	β	σu (kN*m)	β
Pre-corrosion										
B1	6.76	0.975	3.64	0.420	8.45	3.853	0.634	1.01	0.417	1.53
B2	6.57	0.950	3.53	0.411	8.16	5.572	0.932	2.53	0.595	3.96
B3	4.88	0.705	2.36	0.333	4.99	6.328	1.097	2.84	0.728	4.28
Post- corrosion										
B1	5.49	0.791	2.87	0.366	6.20	4.487	0.638	1.99	0.299	4.25
B2	6.12	0.887	3.28	0.395	7.36	4.087	0.610	1.43	0.330	2.64
B3	6.03	0.973	2.89	0.390	7.21	4.545	0.669	1.99	0.342	3.89

With the exception of Beam 3, the reliability indexes also decreased after corrosion. For any given beam and monitoring scheme, the reliability index should decrease along with a reduction in bending moment capacity. However, the asymmetrical conditions that produced the difference in the location of the neutral axis on either side of the beam is believed to have affected the estimation of the effective reinforcing bar area and the remaining bending moment capacity for Beam 3.

5 ECONOMIC ANALYSIS

For the purpose of demonstrating the economic value of implementing an SHM system, the beam was assumed to be an edge beam of a bridge, which is one of the most easily deteriorated structural members of a bridge (Racutanu 1999). Unlike deck slabs, edge beams are generally not protected by waterproof surfacing, so they are more prone to corrosion when exposed to de-icing salt. According to Mattsson et.al (2007), the average replacement cycle for edge beams is 45 years with a standard deviation of 11 years, and the average cost of replacement is $ 820 per meter.

It is assumed that a 45-year old bridge is under inspection, and its edge beams have lost 10% of their reinforcement area due to corrosion. Without further monitoring, a bridge inspector may order the replacement of these beams. In fact, they still have an adequate level of safety based on the reliability analysis using monitored data. Using the post-corrosion analysis for Beam 3 as an example, and assuming the beam will be replaced when the reliability index drops to 2, with Scheme 1, this beam can be allowed to remain in service until its mean bending moment resistance drops to 4.96 kN·m, which corresponds to an effective cross-sectional area of 86%. With Scheme 2, this beam can be allowed to remain in service until its mean bending moment resistance drops to 4.00 kN·m, which corresponds to an effective cross-sectional area of 67%.

The additional service life can be determined based on corrosion rates, which is governed by Faraday's Law:

[2] $M = \frac{WIT}{nF}$

where M is the mass of rust per unit surface area (g/cm^2), W is the atomic weight of steel (56 g/mol), I is the applied current density (A/cm^2), T is the total time that the current has been applied (s), n is the number equivalents exchanged, and F is Faraday's constant (96487 A·s/mol). Under natural conditions, the current density is often between 0.1 to 10 μA/ cm^2 (Malumbela et al. 2012). Since the beam has likely cracked due to 10% corrosion, a high current density of 10 μA/cm^2 can be assumed. On this basis, the replacement of the beam can be delayed for two years with Scheme 1 SHM, and 11 years with Scheme 2 SHM.

The total replacement and monitoring costs associated with 50 m of edge beams, considering a 100-year bridge life span, is illustrated in Figure 6. The total cost of Scheme 1 monitoring equipment is estimated at $2000, assuming that four electrical strain gauges are applied every 2 m, and the cost of each is $20. Scheme 2 has the added cost of a cover meter, which is estimated to be $4,000. Thus, the total cost of Scheme 2 monitoring is $6,000. A discount rate of 5% is used to calculate the present value of total costs for the comparison of different scenarios. Without any monitoring, the present value of total replacement costs is $45,563. On the other hand, the present values of replacement and monitoring costs for Schemes 1 and 2 are $42,942 and $29,971, respectively. The economic value of the two SHM schemes is clear, and the added value associated with the more costly system is realized by the ability of the improved information to delay replacement enough to prevent the need for a second replacement.

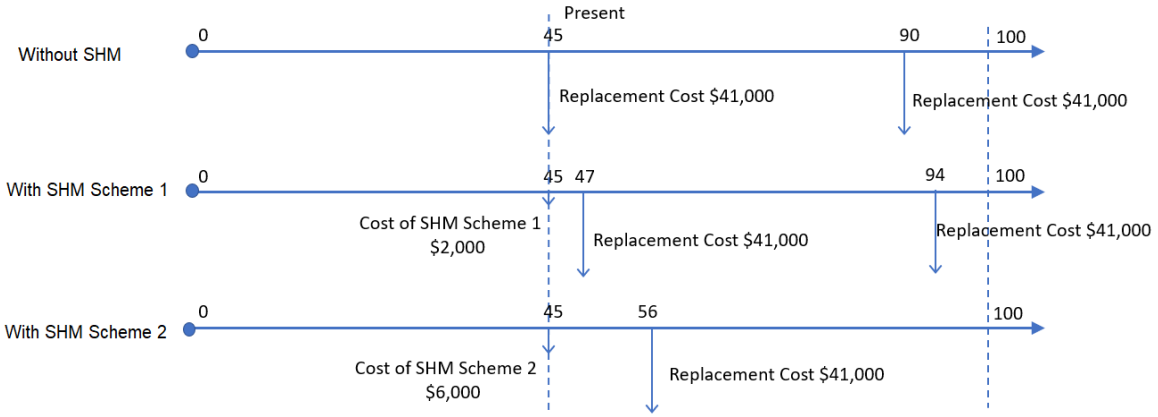

Figure 6: Cashflow of different monitoring conditions

6 CONCLUSIONS

The effectiveness of a strain-based SHM technique for estimating the bending moment capacity of a corroding reinforced concrete beam was evaluated using a laboratory-based experimental study. The results show that the technique has the potential to predict bending moment capacity to within 5% of the measured capacity. When comparing electrical strain gauges to a digital image correlation (DIC) system, data from the electrical strain gauges exhibited lower levels of noise, but they are also constrained by an upper limit on strain. To achieve the best prediction of the remaining cross-sectional area of reinforcing bars, it is recommended that electrical strain gauges be attached on both side surfaces of a beam to minimize the effects of any asymmetry in the system, and that the gauges be located in the compression zone for more reliable measurements. When a cover meter was used to locate the reinforcing bars with greater precision, and this information was combined with data from strain gauges, the reliability index for the same beam in an identical condition was significantly improved. The improved reliability index reflects

a higher level of confidence in structural safety, and thus the structural member can be allowed to remain in service for a longer period of time, until a critical reliability index is reached after additional deterioration. The economic benefit of a more advanced SHM system comes from the extended service life of the structural member and the associated life-cycle cost savings.

References

ASTM 2017. ASTM G1-03 e1 Standard Practice for Preparing, Cleaning, and Evaluating Corrosion Test Specimens, ASTM International, West Conshohocken, PA, USA. www.astm.org

Christensen, P.N., Wegner, L.D., and Sparks, G.A. 2011. Life Cycle Savings of Structural Health Monitoring:A Value of Information Approach. *In Monitoring Technologies for Bridge Management*. *Edited by* B. Bakht, A.A. Mufti, and L.D. Wegner. Multi-science Publishing CO.LTD. pp. 3–31.

Correlated Solutions Inc. 2018. VIC-2D v6 Full-Field Deformation Measurement System. Available from https://www.correlatedsolutions.com/wp-content/uploads/2013/10/VIC-2D-Datasheet.pdf [accessed 25 February 2019].

CSA 2014. *CSA* Standard A23.3-14 Design of Concrete Structures. Canadian Standards Association. Mississauga, Ontario.

Farrar, C.R., and Worden, K. 2007. An introduction to structural health monitoring. *Philosophical transactions. Series A, Mathematical, physical, and engineering sciences*, **365**(1851): 303–15. The Royal Society. doi:10.1098/rsta.2006.1928.

FHWA. 2001. Reliability of Visual Inspection for Highway Bridges, Volume I: Final Report. Available from http://www.tfhrc.gov/hnr20/nde/home.htm [accessed 14 June 2018].

Frangopol, D.M., Messervey, T.B. 2011 Effect of Monitoring on the Reliability of Structures. *In Monitoring Technologies for Bridge Management*. Edited by B. Bakht, A.A. Mufti, and L.D. Wegner. Multi-science Publishing CO.LTD. pp. 515 – 560.

Loupos, K., and Amditis, A. 2017. Structural health monitoring fiber optic sensors. *In Fiber Optic Sensors Current Status and Future Possibilities*. *Edited by* I.R. Matias, S. Ikezawa, and J.C. Editors. Springer International Publishing, Switzerland. pp. 185–206. doi:10.1007/978-3-319-42625-9_9.

Malumbela, G., Moyo, P., and Alexander, M. 2012. A step towards standardising accelerated corrosion tests on laboratory reinforced concrete specimens. *Journal of the South African Institution of Civil Engineering*, **54**(2): 78–85.

Mattsson, H.-Ä., Sundquist, H., and Silfwerbrand, J. 2007. The Real Service Life and Repair Costs for Bridge Edge Beams. *Restoration of Buildings and Monuments*, **13**(4): 215–228. De Gruyter. doi:10.1515/rbm-2007-6140.

Proceq. 2007. RebaR detection system. Available from http://infrastruct.ie/wp-content/uploads/2013/04/Proceq-Profometer-5+.pdf [accessed 21 May 2018].

Qin, J., Thöns, S., and Faber, M.H. 2015. On the value of SHM in the context of service life integrity management. *Proceedings of the 12th International Conference on Applications of Statistics and Probability in Civil Engineering*,. Vancouver, Canada. doi:10.14288/1.0076291.

Racutanu, G. 1999. The Real Service Life of Road Bridges in Sweden - A Case Study. *In Durability of Building Materials and Components 8. Edited by* M.A. Lacasse and D.J. Vanier. Institure for Research in Construction, Ottawa ON. pp. 56–70. Available from https://www.irbnet.de/daten/iconda/CIB2042.pdf [accessed 24 February 2019].

Rytter, A. 1993. Vibrational Based Inspection of Civil Engineering Structures. Dept. of Buliding Technology and Structural Engineering, Aalborg University. Available from http://vbn.aau.dk/files/18588667/Vibrational_Based_Inspection_of_Civil_Engineering_Structures [accessed 20 May 2018].

Yan, S., Ma, H., Li, P., Song, G., and Wu, J. 2017. Development and Application of a Structural Health Monitoring System Based on Wireless Smart Aggregates. *Sensors,* Basel, Switzerland, **17**(7). Multidisciplinary Digital Publishing Institute (MDPI). doi:10.3390/s17071641.

Zhang, W., Zhang, R., Xi, L., Ruiyuan, Z., and Lijuan, X. 2013. Corrosion of reinforced concrete in accelerated tests. *Advanced Materials Research*, **610–613**: 485–489. doi:10.4028/www.scientific.net/AMR.610-613.485.